



Shape Coherence and Finite-Time Curvature Evolution

Tian Ma* and Erik M. Bollt†

*Department of Mathematics and Computer Science,
Clarkson University, USA*

**mat@clarkson.edu*

†bolltem@clarkson.edu

Received December 17, 2014

We introduce a definition of finite-time curvature evolution along with our recent study on shape coherence in nonautonomous dynamical systems. Comparing to slow evolving curvature preserving the shape, large curvature growth points reveal the dramatic change on shape such as the folding behaviors in a system. Closed trough curves of low finite-time curvature (FTC) evolution field indicate the existence of shape coherent sets, and troughs in the field indicate the most significant shape coherence. Here, we will demonstrate these properties of the FTC, as well as contrast to the popular Finite-Time Lyapunov Exponent (FTLE) computation, often used to indicate hyperbolic material curves as Lagrangian Coherent Structures (LCS). We show that often the FTC troughs are in close proximity to the FTLE ridges, but in other scenarios, the FTC indicates entirely different regions.

Keywords: Shape coherence; finite-time curvature; finite-time stable and unstable foliation.

1. Introduction

Coherence has clearly become a central concept of interest in nonautonomous dynamical systems, particularly in the study of turbulent flows, with many recent papers designed toward describing, quantifying and constructing such sets [Ma & Bollt, 2014; Haller & Beron-Vera, 2012; Froyland *et al.*, 2010; Ma & Bollt, 2013; Froyland & Padberg, 2009; Kelley & Ouellette, 2011a; Tallapragada & Ross, 2013]. There have been a wide range of notions of coherence, from spectral [Holmes *et al.*, 1998], to set oriented [Dellnitz *et al.*, 2001] and through transfer operators [Froyland & Padberg, 2009; Froyland *et al.*, 2010] as well as variational principles [Meiss, 1992], and even topological methods [Allshouse & Thiffeault, 2012; Grover *et al.*, 2012]. Traditionally there has been an emphasis on vorticity [Hussain, 1986], but generally an understanding that, coherent motions have a role in maintenance (production and dissipation) of turbulence in a boundary layer [Robinson, 1991]. A number of theories have been

developed to model and analyze the dynamics in the Lagrangian perspective (moving frame), such as the geodesic transport barriers [Haller & Beron-Vera, 2012] and transfer operators method [Froyland *et al.*, 2010]. These have included the analysis of coherence in important problems such as how regions of fluids are isolated from each other [Allshouse & Thiffeault, 2012] including in the prediction of oceanic structures [Froyland *et al.*, 2007] and atmospheric forecasting [BozorgMagham & Ross, 2015; BozorgMagham *et al.*, 2013], especially for understanding the movement of pollution including such as oil spills [Olascoaga & Haller, 2012; Mezic *et al.*, 2010; Bollt *et al.*, 2012]. Whatever the perspectives taken, we generally interpretively summarize that coherent structures can be taken as a region of simplicity, within the observed time scale and stated spatial scale, perhaps embedded within an otherwise possibly turbulent flow [Haller & Beron-Vera, 2012; Froyland *et al.*, 2010; Froyland & Padberg, 2009; Ma & Bollt, 2014].

In particular, the ridges from Finite-Time Lyapunov Exponents (FTLE) fields have been widely used [Haller, 2000, 2002; Shadden *et al.*, 2005; Talapragada & Ross, 2013] to indicate hyperbolic material curves, often called Lagrangian coherent structures (LCS). We contrast here the fundamental nonlinear notions of “stretching” encapsulated in the FTLE concept to “folding” which is a complementary concept of a nonlinear dynamical system which must be present if a material curve can stretch indefinitely within a compact domain. We will show that exploring the much-overlooked folding concepts leads to developing curvature changes of material curves yielding an elegant description of coherence that we call shape coherence [Ma & Boltt, 2013]. We introduce here a method of visualizing propensity of a material curve to change its curvature, which we call the Finite-Time Curvature (FTC) field. Contrasting the FTC to the FTLE, we will illustrate that sometimes the FTC troughs indicative of shape coherence are often co-mingled in close proximity to ridges of the FTLE, and in such cases, they indicate a generally similar story. However, we show that in many cases, the FTC troughs occur in locations not near an FTLE ridge, indicating entirely different regions. Thus, we view these as complementary concepts, stretch and fold, as revealed by the traditional FTLE and here introduced FTC.

2. Shape Coherence

We have recently presented a mathematical interpretation of coherence [Ma & Boltt, 2013] in terms of the definition of *shape coherent sets*, motivated by a simple observation regarding sets that “hold together” over finite-time in nonautonomous dynamical systems. As a general setup, assume an area preserving system that can be represented,

$$\dot{z} = g(z, t), \quad (1)$$

for $z(t) \in \mathbb{R}^2$, with enough regularity of g so that a corresponding flow, $\Phi_T(z_0) : \mathbb{R} \times \mathbb{R}^2 \rightarrow \mathbb{R}^2$, exists. To capture the idea of a set that roughly preserves its own shape, we define [Ma & Boltt, 2013] the *shape coherence factor* α between two sets A and B under an area preserving flow Φ_t over a finite time interval $[0, T]$,

$$\alpha(A, B, T) := \sup_{S(B)} \frac{m(S(B) \cap \Phi_T(A))}{m(B)}, \quad (2)$$

where $m(\cdot)$ here denotes Lebesgue measure, and we restrict the domain of α to sets such that $m(B) \neq 0$ by assumptions to follow that B should be a fundamental domain [Ahlfors, 1979]. Here, $S(B)$ is the group of transformations of rigid body motions of B , specifically translations and rotations descriptive of *frame invariance* [do Carmo, 1976], and for certain problems including mirror translations is appropriate. We say A is finite time shape coherent to B with shape coherence factor α , under the flow Φ_T after time epoch T . We call B the *reference set*, and A shall be called the *dynamic set*. If we choose $B = A$, we can verify to what degree a set A preserves its shape over the time epoch T . Notice that the shape of A may vary during the time interval, but for a high shape coherence, the shapes must be similar at the terminal times. By the area preserving assumption, $0 \leq \alpha \leq 1$, and values closer to 1 indicate a set for which the otherwise nonlinear flow restricted to A is much simpler, at least on the time scale T and on the spatial scale corresponding to A ; that is $\Phi_T|_A$, the flow restricted to A is roughly much simpler than a turbulent system, as it is much more like a rigid body motion. This does not preclude on finer scales, that there may be turbulence within a shape coherent set.

2.1. Curvature evolution

Recall that for any material curve, $\gamma(s, t) = (x_1(s, t), x_2(s, t))$ of initial conditions defining an initial segment $\gamma(s, 0) = (x_1(s, 0), x_2(s, 0))$, $a \leq s \leq b$ where each point on the curve evolves in time t according to the differential equation, the curvature at time t may be written in terms of the parametric derivative along the curve segment, $d/ds := ' ,$

$$k(s, t) = \frac{|x_1'x_2'' - x_2'x_1''|}{(x_1'^2 + x_2'^2)^{3/2}}. \quad (3)$$

We will relate the pointwise changes of this curvature function for points on those material curves that correspond to shape coherence.

The analysis of the geometry of shape coherent sets A depends on the boundary of these sets, ∂A , which we restrict in the following to simply connected sets such that the boundary is a smooth and simple closed curve, $\partial A = \gamma(s), 0 \leq s \leq 1$, and these are often called “fundamental domains” [Ahlfors, 1979]. These $B = A$ are in the domain of α . We may relate shape coherence

to the classical differential geometry whereby two curves are defined to be congruent if their underlying curvature functions can be exactly matched, pointwise [do Carmo, 1976]. Therefore, considering the Frenet–Serret formula [do Carmo, 1976], it can be proved [Ma & Boltt, 2014] through a series of regularity theorems that those sets with a slowly evolving propensity to change curvature correspond to boundaries of sets with a significant degree of shape coherence. That is $\alpha(A, \Phi_T(A)) \approx 1$.

Furthermore, a sufficient condition theorem connects geometry that points z where there is a tangency between finite-time stable and unstable foliations $f_u^t(z)$, $f_s^t(z)$ must correspond to slowly changing curvature. In Fig. 1, we indicate the geometry of stable and unstable foliations that correspond to tangency or near tangency where curves passing through such points experience slowly changing curvature, and hence indicative of points on the boundaries of shape coherent sets [Ma & Boltt, 2014]. Hence, finding shape coherent sets leads us to the search for curves of tangency points as the boundaries of such set which we review below. Much has been written about the role of how stable and unstable manifolds can become reversed at tangency points in that errors can grow transversely to the unstable manifolds as noted in [Kantz & Schreiber, 2004; Boltt *et al.*, 2001; Zyczkowski & Boltt, 1999]. Scaling relationships for frequency of given curvatures in [Thiffeault, 2004, 2002; Thiffeault & Allen, 2001; Liu & Muzzio, 1996; Drummond & Munch, 1991; Drummond, 1993; Pope *et al.*, 1989; Ishihara & Kaneda, 1992], as well as the propensity of curvature growth in turbulent systems [Ouellette & Gollub, 2007, 2008; Kelley & Ouellette, 2011a; Xu *et al.*, 2007] have both been studied.

2.2. Finite-time stable and unstable foliations

Recall that finite-time stable foliation $f_s^t(z)$ at z describes the dominant direction of local contraction in forward time, and unstable foliation $f_u^t(z)$ describes dominant direction of contraction in “backward” time. Traditionally, these particularly relate to Lyapunov exponents and directions [Geist *et al.*, 1990; Boltt & Santitissadeekorn, 2013], and lately in [Haller & Beron-Vera, 2012]. See Fig. 1. The derivative, $D\Phi_t(z)$ maps a circle onto an ellipse, as does any general matrix [Berger, 1987]. The infinitesimal geometry of a small disc of variations from $\Phi_t(z)$ is shown in Fig. 1. Likewise, a disc centered on $\Phi_t(z)$ pulls back under $D\Phi_{-t}(\Phi_t(z))$ to an ellipsoid centered on z . The major axis of that ellipsoid defines $f_s^t(z)$. Likewise, from $\Phi_{-t}(z)$, variations push forward under $D\Phi_t(\Phi_{-t}(z))$, the major axis of which defines, $f_u^t(z)$. These major axis can be readily computed by SVD [Golub & Loan, 1996] of derivative matrices, as noted for Lyapunov directions [Geist *et al.*, 1990; Boltt & Santitissadeekorn, 2013; Oseledets, 1968] and recently [Karrasch, 2014]. Let,

$$D\Phi_t(z) = U\Sigma V^T \quad (4)$$

and U and V are orthogonal matrices, $V = [v_1, v_2]$, and $U = [u_1, u_2]$. Note that

$$D\Phi_t(z)v_1 = \sigma_1 u_1, \quad (5)$$

describes the vector v_1 at z that maps onto the major axis $\sigma_1 u_1$ at $\Phi_t(z)$. Since

$$\Phi_{-t} \circ \Phi_t(z) = z \quad \text{and} \quad D\Phi_{-t}(\Phi_t(z))D\Phi_t(z) = I, \quad (6)$$

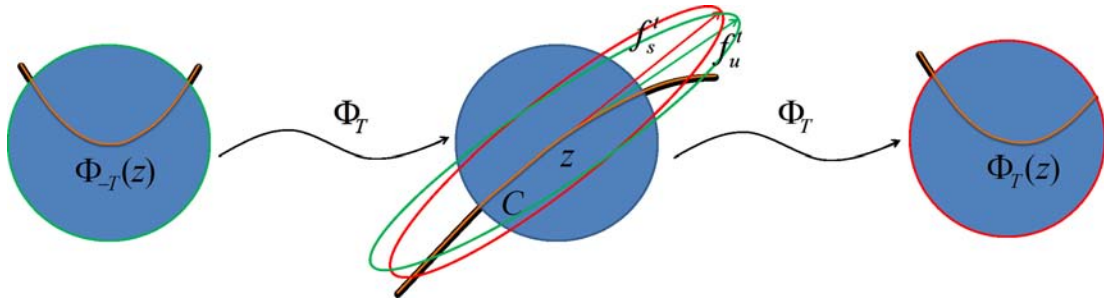


Fig. 1. Tangency points of stable and unstable foliations are highlighted as at such points, infinitesimal curve elements experience curvature that terminally evolves slowly in the time epoch. Notice that the stable foliation $f_s^T(z)$ is the major axis of preimage of variations from $\Phi_T(z)$ and correspondingly $f_u^T(z)$ is the major axis of image of variations from $\Phi_{-T}(z)$.

then orthogonally, we get

$$D\Phi_{-t}(\Phi_t(z)) = V\Sigma^{-1}U^T \quad (7)$$

and

$$\Sigma^{-1} = \text{diag}\left(\frac{1}{\sigma_1}, \frac{1}{\sigma_2}\right) \quad (8)$$

and the dominant axis from $\Phi_t(z)$ follows,

$$D\Phi_t(z)u_2 = \frac{1}{\sigma_2}v_2. \quad (9)$$

Hence,

$$f_s^t(z) = v_2 \quad \text{and} \quad f_u^t(z) = \bar{u}_1, \quad (10)$$

where $D\Phi_t(z) = U\Sigma V^T$ and likewise, \bar{u}_1 is the first left singular vector of $D\Phi_t(\Phi_{-t}(z)) = \bar{U}\bar{\Sigma}\bar{V}^*$.

2.3. Example: Rossby wave

We choose the Rossby wave [Rypina *et al.*, 2007] system, an idealized zonal stratospheric flow, for further presentation. Consider the Hamiltonian system $dx/dt = -\partial H/\partial y$, $dy/dt = \partial H/\partial x$, where

$$\begin{aligned} H(x, y, t) = & c_3y - U_0L \tanh\left(\frac{y}{L}\right) \\ & + A_3U_0L \text{sech}^2\left(\frac{y}{L}\right) \cos(k_1x) \\ & + A_2U_0L \text{sech}^2\left(\frac{y}{L}\right) \cos(k_2x - \sigma_2t) \\ & + A_1U_0L \text{sech}^2\left(\frac{y}{L}\right) \cos(k_1x - \sigma_1t). \end{aligned} \quad (11)$$

In Fig. 2(a) we show simultaneously the stable and unstable foliation fields, $f_s^t(z)$ and $f_u^t(z)$, of this system, together with curves of zero-angle [Fig. 2(b)], $\theta(z, t) = 0$, where

$$\theta(z, t) := \arccos \frac{\langle f_s^t(z), f_u^t(z) \rangle}{\|f_s^t(z)\| \|f_u^t(z)\|}, \quad (12)$$

found by implicit function theorem as described in [Ma & Bollt, 2014], corresponding to significant shape coherence. The main work of this paper therefore is to show that this detail can be skipped as the FTC we introduce significantly simplifies the geometry and facilitates the computation.

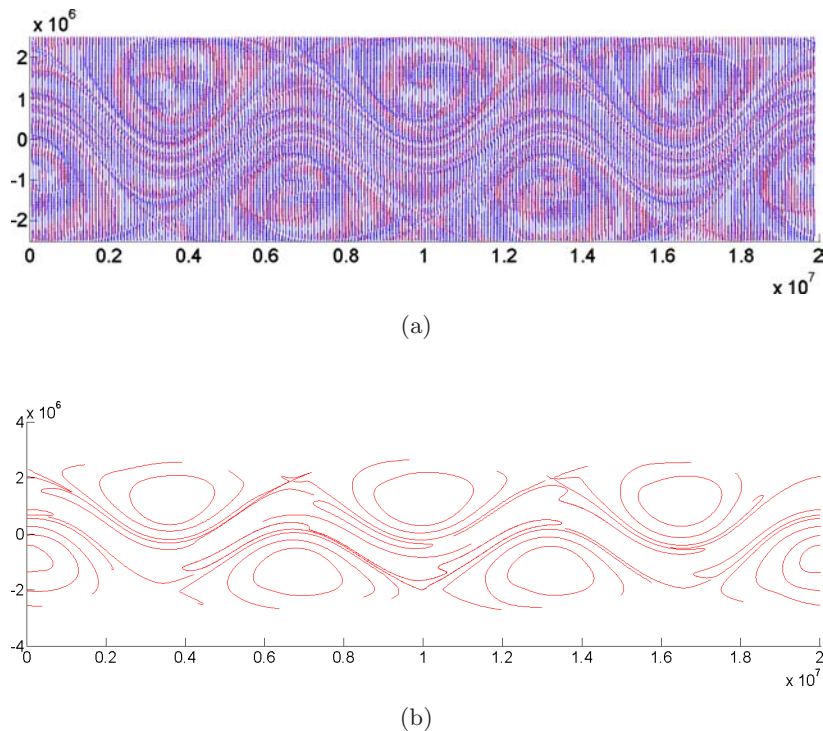


Fig. 2. (a) The finite-time stable and unstable foliation fields $f_s^t(z)$ and $f_u^t(z)$ for the Rossby wave system. Notice that for each point, there are two vectors, and therefore an associated angle $\theta(z, t)$. (b) Zero-splitting curves corresponding to boundaries of shape coherent sets corresponding to a significant shape coherence factor, Eq. (2). The parameters are set, $U_0 = 44.31$, $c_2 = 0.2055U_0$, $c_3 = 0.462U_0$, $A_3 = 0.3$, $A_2 = 0.12$, $A_1 = 0.075$ [Rypina *et al.*, 2007], and time epoch $T = 10$ days. (a) Foliation field and (b) nonhyperbolic splitting curves.

3. Finite-Time Curvature Field

Here we introduce a simplified analysis and construction of shape coherence by direct measurement and display of fields of maximal rate of change of any possible curvature, which we call the Finite-Time Curvature field (FTC). The FTC allows us to interpret sets of significant shape coherence, by direct inspection of those points and curves corresponding to slowly evolving curvature, with the interpretation cited above to the theorems connecting shape coherence to the slow evolution of boundary curvature.

3.1. Definition of finite-time curvature fields

The intuition behind the FTC development is based on the idea that the folding behaviors involve the maximal propensity of changing curvature. This suggests that regions of space corresponding to slowly changing curvature include boundaries of significant shape coherence. We define the *maximum finite-time curvature (maxFTC)*, $C_{t_0}^{t_0+\tau}(z)$, and *minimum finite-time curvature (minFTC)*, $c_{t_0}^{t_0+\tau}(z)$, for a point z in the plane under a flow $\Phi_{t_0}^{t_0+\tau}$ over the time interval $[t_0, t_0 + \tau]$ by,

$$C_{t_0}^{t_0+\tau}(z) = \lim_{\epsilon \rightarrow 0} \sup_{\|v\|=1} \kappa(\Phi_{t_0}^{t_0+\tau}(l_{\epsilon,v}(z))), \quad (13)$$

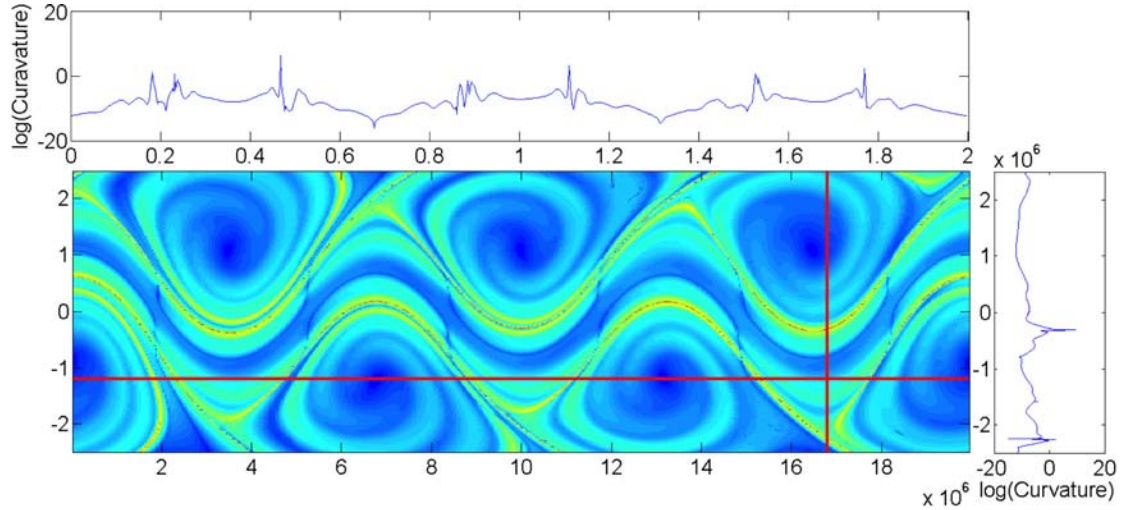
$$c_{t_0}^{t_0+\tau}(z) = \lim_{\epsilon \rightarrow 0} \inf_{\|v\|=1} \kappa(\Phi_{t_0}^{t_0+\tau}(l_{\epsilon,v}(z))) \quad (14)$$

where,

$$l_{\epsilon,v}(z) := \{\hat{z} = z + \epsilon sv, |s| < 1\} \quad (15)$$

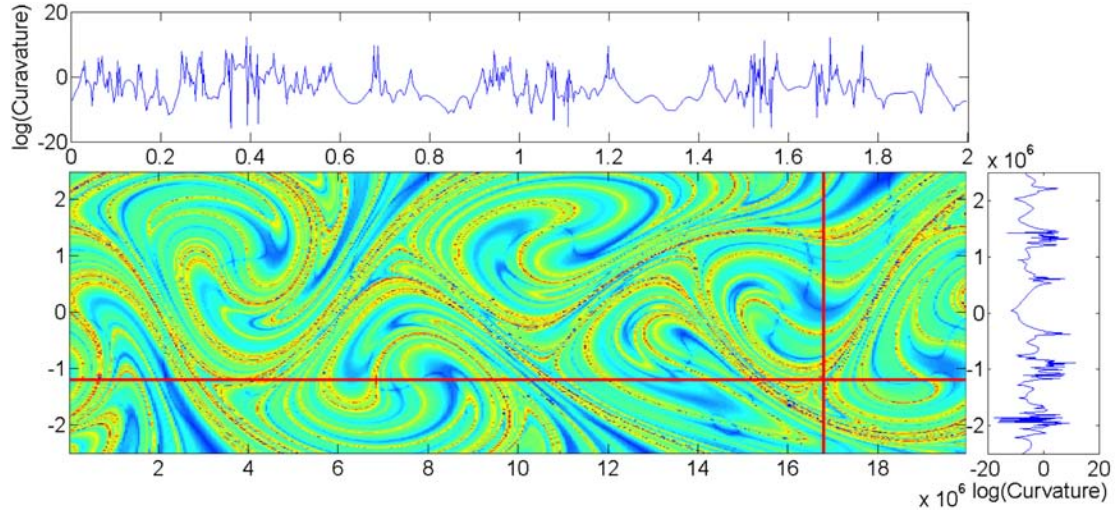
and v is a unit vector, and $l_{\epsilon,v}(z)$ is a small line segment passing through the point $z = (x, y)$, when $\epsilon \ll 1$. These will always exist, so defined in terms of sup and inf. When Φ is sufficiently smooth, then κ will be continuous and the above formula can be maximized traditionally, for example, by gradient descent with respect to the angle of the unit vector v , and in practice, we estimate the limit by small ϵ . Also, here we are generally interested in the maxFTC, and as such, we will often refer to it simply as the FTC field.

Generally, when the maxFTC has a trough (curve) of small values, then this suggests that there is a strong nonhyperbolicity such as an elliptic island boundary or some other form of tangency as displayed in Fig. 1. These are darker blue “FTC trough curves” as seen in Fig. 3(a), that serve as boundaries between shape coherent sets. These curves can approximately maintain their shape for



(a)

Fig. 3. (a) Shows the maxFTC fields $C_{t_0}^{t_0+\tau}(z)$ of different groups of parameters of the Rossby wave system. Note that in both figures, the level curves of relatively smaller maxFTC, $C_{t_0}^{t_0+\tau}(z)$ from Eq. (13), indicate that there exist material curves whose curvature changes slowly (blue curves) and these correspond to the zero-splitting curves in Fig. 2 [Ma & Boltt, 2014]. On the top and sides of (a) and (b) we show a slice of the maxFTC function along the red lines shown respectively. Large variation indicates boundaries of shape coherent sets. Boundaries are indicated by low values of the maxFTC, small propensity to grow curvature. Fast variation at boundaries indicates high curvature change is often closely proximal to low curvature change, indicative within the (hetero)homoclinic tangle where tangencies and hyperbolicity often coexist. Compare to partition developed in Fig. 4. (a) maxFTC $U_0 = 44.31$, $c_3 = 0.461U_0$, $A_3 = 0.3$ and (b) maxFTC $U_0 = 63.66$, $c_3 = 0.7U_0$, $A_3 = 0.2$.



(b)

Fig. 3. (Continued)

relatively longer time. However, the largest ridges of the maxFTC illustrate points where there are both significant curvature growth along one direction but small transverse curvature growth, when there is an area preservation assumption. These level curves arise in the scenario of the sharply changing curvature developing at the most extreme points in a (hetero)homoclinic tangle, as illustrated in Fig. 1. Notice that the FTC trough curves can be used to estimate shape coherent sets. A particularly interesting feature of these FTC fields is the large variation in certain regions, indicated at the top and on the side of Figs. 3(a) and 3(b); this is clearly due to co-located hyperbolicity and nonhyperbolicity regions of (hetero)homoclinic tangles, discussed in greater detail in comparison to FTLE in Fig. 5. The FTC field in Figs. 3(a) and 3(b) clearly suggests boundaries of the shape coherent sets as low

(blue) troughs, as discussed below and emphasized by the partition shown in Fig. 4.

3.2. Relationship of FTC to shape coherence

To construct shape coherent sets from the FTC, we describe two complementary perspectives. One follows the idea of curve continuation by the implicit function theorem, but on the FTC to track level curves of $r_{t_0}^{t_0+\tau}(z)$. That is, if a point z_0 where a (near) minimal value $r_{t_0}^{t_0+\tau}(z) = R$ is found, representing a point in the trough, then other values nearby can be derived by

$$z' = h(z) = -\frac{\frac{\partial(r_{t_0}^{t_0+\tau})}{\partial y}}{\frac{\partial(r_{t_0}^{t_0+\tau})}{\partial x}}(z), \quad (16)$$

as an ordinary differential equation with initial condition $z(0) = z_0$, and the derivative $' = \frac{d}{ds}$ represents the variation along the s -parameterized arc. Furthermore, by the above principle of component analysis, the directions of maximal curvature are also encoded in the principle vectors of $D\Phi_t(z)$.

A direct search for the interiors of sets between low troughs of the FTC is a problem of defining regions between boundary curves, and this relates to a common problem of image processing called image segmentation [Yoo, 2004].

In particular, we applied the diffusion-like “seeded region growing” method [Adams & Bischof,

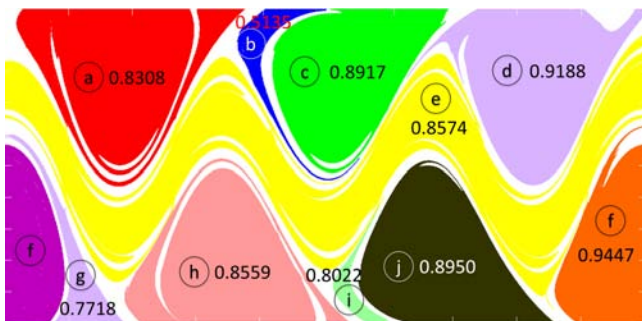


Fig. 4. The partition of the Rossby wave system from diffusion-like “seeded region growing” method of the FTC seen in Fig. 3. Numbers adjacent to each letter a–j indicate the shape coherence $\alpha(A, \Phi_T(A), T)$ of the set shown.

1994] that begins by selecting a set of seed points. Here, we apply 100 uniform grid points as seeds and use four connected neighborhoods to grow from the seed points. We slightly improve a well regarded

implementation that can be found in [Kroon, 2008]. See Fig. 4 for the partitioning results. Several shape coherent sets corresponding to Fig. 3 are found. Specifically, the middle yellow band has

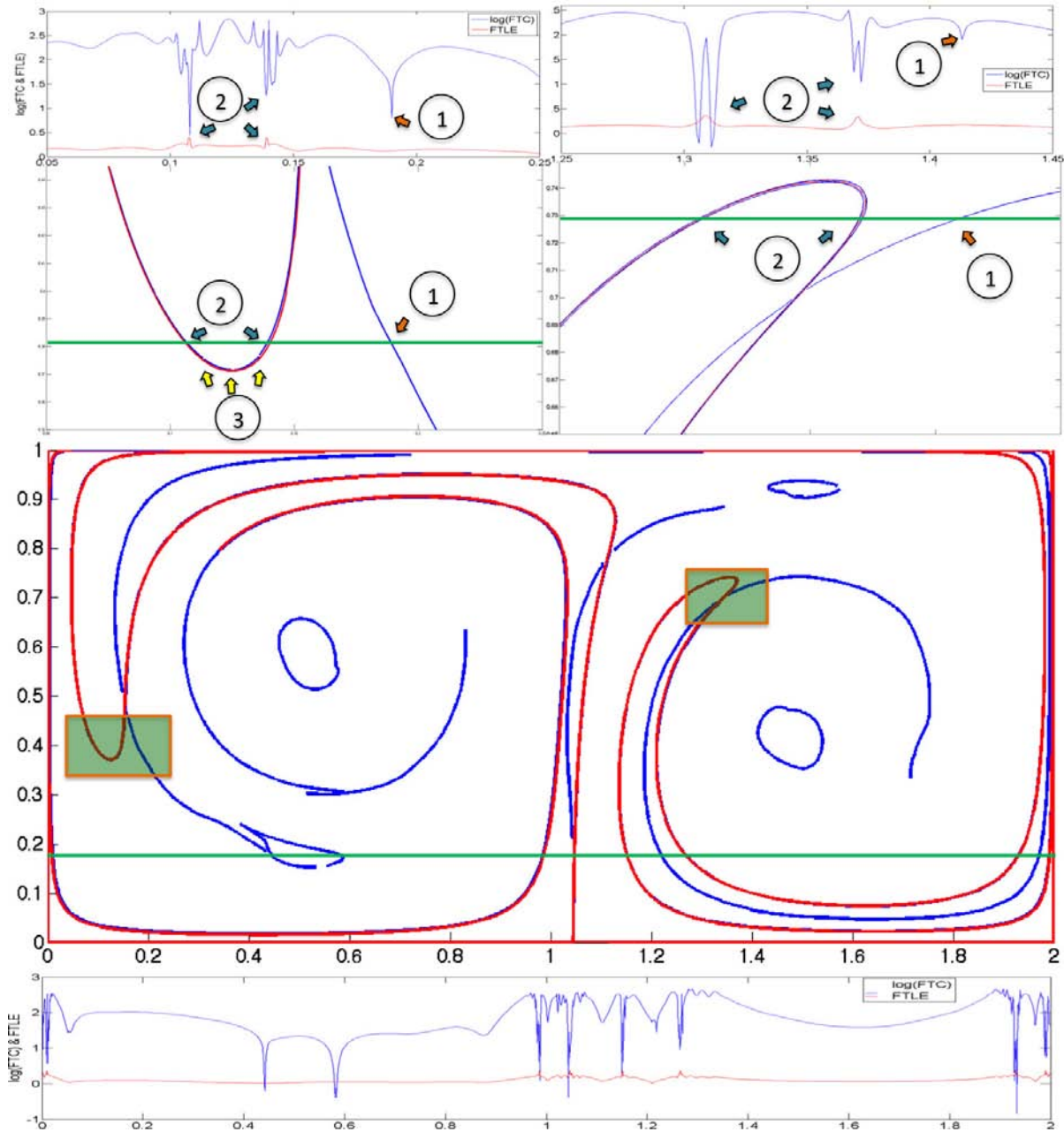


Fig. 5. The FTC troughs of the double gyre highlighted in blue, and FTLE ridges highlighted in red, are seen to be sometimes in close proximity. Thus similar regions are indicated. However, they are often not near each other indicating disparate regions. In the blow-up insets above, we see labels “2” indicate where the FTLE ridges are in-between FTC troughs, and likewise the one-dimensional slice along the green curve shows these field values on a log scale repeating this outcome. Lows of the blue curve are near but offset slightly highs of the red curve, often, highs of the blue field surrounding lows of the red field. At such locations the two disparate computations reveal similar dynamics. However, regions indicated by “1” reveal FTC-trough curves which are entirely separated from any FTLE behavior of interest. Thus a different outcome is found at such locations. Closed curves of FTC-troughs indicate shape coherence. At regions indicated by “3” we see gaps in the FTC curves. At the bottom we show a slice of the FTC and FTLE curves through the full phase space.

$\alpha(A, \Phi_T(A), T) = 0.8574$, and likewise the α -values of the remaining colored sets are shown in Fig. 4. Some difference in the otherwise symmetric regions are due to the region clipping as shown.

3.3. An example of comparison between FTC and FTLE: Double gyre

Finally, we contrast results from the FTC field versus the highly popular FTLE field [Shadden *et al.*, 2005] since at first glance, the pictures may seem essentially similar, despite the significantly different definitions and different perspectives. Recall [Shadden *et al.*, 2005] that the FTLE is defined pointwise over a time epoch- t that

$$L_t(z) = \frac{1}{t} \log \sqrt{\rho(D\Phi'_t(z)D\Phi_t(z))}, \quad (17)$$

where ρ is the largest eigenvalue of the Cauchy–Green strain tensor. In the following, we contrast FTLE and FTC in the context of what follows the nonautonomous Hamiltonian,

$$\begin{aligned} \dot{x} &= -\pi A \sin(\pi f(x, t)) \cos(\pi y) \\ \dot{y} &= \pi A \cos(\pi f(x, t)) \sin(\pi y) \frac{df}{dx} \end{aligned} \quad (18)$$

where $f(x, t) = \epsilon \sin(\omega t)x^2 + (1 - 2\epsilon \sin(\omega t))x$, $\epsilon = 0.1$, $\omega = 2\pi/10$ and $A = 0.1$, which has become a benchmark problem [Shadden *et al.*, 2005]. Observe in Fig. 5 that sometimes an FTC trough indicative of shape coherence may occur spatially in close proximity to an FTLE ridge indicative of high finite time hyperbolicity [Haller & Beron-Vera, 2012; Shadden *et al.*, 2005] and thus suggests a transport pseudo-barrier [Haller & Beron-Vera, 2012; Shadden *et al.*, 2005]. It is true that folding often occurs in close proximity to regions of strong hyperbolic stretching [Thiffeault, 2004, 2002; Thiffeault & Allen, 2001], as already hinted by the fast variations of FTC in hyperbolic regions as seen in the traces on the tops and the sides of Figs. 3(a) and 3(b). However, in Fig. 5, we directly address the coincidences and differences, by locating the troughs of the FTC shown as blue curves, and the ridges of the FTLE shown as red curves. Clearly sometimes FTC troughs find curves close to FTLE ridges, but at times, entirely new curves are found. When the FTC troughs are closed, shape coherent sets are indicated, and are not found in any other

way when not near the FTLE. Finally note that as indicated by “3” in Fig. 5, where the FTLE curves may have a strong curvature, those FTC may be in close parallel, but the FTC trough curves may have breaks as indicated.

4. Conclusion

With these coincidences, and given differences in definitions, concepts and results, we have offered here the FTC as a new concept for interpreting shape coherence in turbulent systems, that results in a decomposition of chaotic systems into regions of simplicity, and by complement regions of complexity. There is the promised implications that we plan to study further, between shape coherence and persistence of energy and enstrophy along Lagrangian trajectories as was previously studied in the context of FTLE [Kelley & Ouellette, 2011b].

Acknowledgment

This work was supported by the Office of Naval Research.

References

- Adams, R. & Bischof, L. [1994] “Seeded region growing,” *IEEE Trans. Patt. Anal. Mach. Intell.* **16**, 641–647.
- Ahlfors, L. [1979] *Complex Analysis* (McGraw-Hill Science), pp. 98–99.
- Allhouse, M. & Thiffeault, J. L. [2012] “Detecting coherent structures using braids,” *Physica D* **241**, 95–105.
- Berger, M. [1987] *Geometry I* (Springer, Berlin).
- Bollt, E. M., Stanford, T., Lai, Y. C. & Zyczkowski, K. [2001] “What symbolic dynamics do we get with a misplaced partition? On the validity of threshold crossings analysis of chaotic time-series,” *Physica D* **154**, 259–286.
- Bollt, E. M., Luttmann, A., Kramer, S. & Basnayake, R. [2012] “Measurable dynamics analysis of transport in the gulf of mexico during the oil spill,” *Int. J. Bifurcation and Chaos* **22**, 1230012.
- Bollt, E. M. & Santitissadeekorn, N. [2013] *Applied and Computational Measurable Dynamics* (Society for Industrial and Applied Mathematics).
- BozorgMagham, A. E., Ross, S. D. & Schmale, III, D. G. [2013] “Real-time prediction of atmospheric Lagrangian coherent structures based on forecast data: An application and error analysis,” *Physica D* **258**, 47–60.
- BozorgMagham, A. E. & Ross, S. D. [2015] “Atmospheric Lagrangian coherent structures considering

- unresolved turbulence and forecast uncertainty,” *Commun. Nonlin. Sci. Numer. Simul.* **22**, 964–979.
- Dellnitz, M., Froyland, G. & Junge, O. [2001] “The algorithms behind GAIO — Set oriented numerical methods for dynamical systems,” *Ergodic Theory, Analysis, and Efficient Simulation of Dynamical Systems* (Springer, Berlin, Heidelberg), pp. 145–174.
- do Carmo, M. P. [1976] *Differential Geometry of Curves and Surfaces* (Pearson).
- Drummond, I. T. & Munch, W. [1991] “Distortion of line and surface elements in model turbulent flows,” *J. Fluid Mech.* **225**, 529–543.
- Drummond, I. T. [1993] “Stretching and bending of line elements in random flows,” *J. Fluid Mech.* **252**, 479–498.
- Froyland, G., Padberg, K., England, M. H. & Treguier, A. M. [2007] “Detection of coherent oceanic structures via transfer operators,” *Phys. Rev. Lett.* **98**, 224503.
- Froyland, G. & Padberg, K. [2009] “Almost-invariant sets and invariant manifolds — Connecting probabilistic and geometric descriptions of coherent structures in flows,” *Physica D* **238**, 1507–1523.
- Froyland, G., Santitissadeekorn, N. & Monahan, A. [2010] “Transport in time-dependent dynamical systems: Finite-time coherent sets,” *Chaos* **20**, 043116.
- Geist, K., Parlitz, U. & Born, W. L. [1990] “Comparison of different methods for computing Lyapunov exponents,” *Progr. Theoret. Phys.* **83**, 875–893.
- Golub, G. H. & Loan, C. F. V. [1996] *Matrix Computations* (Johns Hopkins University Press).
- Grover, P., Ross, S. D., Stremler, M. A. & Kumar, P. [2012] “Topological chaos, braiding and bifurcation of almost-cyclic sets,” *Chaos* **22**, 043135.
- Haller, G. [2000] “Finding finite-time invariant manifolds in two-dimensional velocity fields,” *Chaos* **10**, 99.
- Haller, G. [2002] “Lagrangian coherent structures from approximate velocity data,” *Phys. Fluids* **14**, 1851.
- Haller, G. & Beron-Vera, F. J. [2012] “Geodesic theory of transport barriers in two-dimensional flows,” *Physica D* **241**, 1680–1702.
- Holmes, P., Lumley, J. L. & Berkooz, G. [1998] *Turbulence, Coherent Structures, Dynamical Systems and Symmetry* (Cambridge University Press).
- Hussain, A. K. M. F. [1986] “Coherent structures and turbulence,” *J. Fluid Mech.* **173**, 303–356.
- Ishihara, T. & Kaneda, Y. [1992] “Stretching and distortion of material line elements in two-dimensional turbulence,” *J. Phys. Soc. Japan* **61**, 3547.
- Kantz, H. & Schreiber, T. [2004] *Nonlinear Time Series Analysis* (Cambridge University Press).
- Karrasch, D. [2014] “On attracting Lagrangian coherent structures,” arXiv:1311.5043v4.
- Kelley, D. H. & Ouellette, N. T. [2011a] “Separating stretching from folding in fluid mixing,” *Nat. Phys.* **7**, 477–480.
- Kelley, D. H. & Ouellette, N. T. [2011b] “Spatiotemporal persistence of spectral fluxes in two-dimensional weak turbulence,” *Phys. Fluids* **23**, 115101.
- Kroon, D. J. [2008] <http://www.mathworks.com/matlabcentral/fileexchange/19084-region-growing>.
- Liu, M. & Muzzio, F. J. [1996] “The curvature of material lines in chaotic cavity flows,” *Phys. Fluids* **8**, 75.
- Ma, T. & Bollt, E. M. [2013] “Relatively coherent sets as a hierarchical partition method,” *Int. J. Bifurcation and Chaos* **23**, 1330026-1–17.
- Ma, T. & Bollt, E. M. [2014] “Differential geometry perspective of shape coherence and curvature evolution by finite-time nonhyperbolic splitting,” *SIAM J. Appl. Dyn. Syst. (SIADS)* **13**, 1106–1136.
- Meiss, J. D. [1992] “Symplectic maps, variational principles, and transport,” *Rev. Mod. Phys.* **64**, 795.
- Mezic, I., Loire, S., Fonoberov, V. A. & Hogan, P. [2010] “A new mixing diagnostic and gulf oil spill movement,” *Science* **330**, 486–489.
- Olascoaga, M. J. & Haller, G. [2012] “Forecasting sudden changes in environmental pollution patterns,” *Proc. Natl. Acad. Sci. USA* **109**, 4738–4743.
- Oseledets, V. I. [1968] “Multiplicative ergodic theorem: Characteristic Lyapunov exponents of dynamical systems,” *Rudy MMO* **19**.
- Ouellette, N. T. & Gollub, J. P. [2007] “Curvature fields, topology, and the dynamics of spatiotemporal chaos,” *Phys. Rev. Lett.* **99**, 194502.
- Ouellette, N. T. & Gollub, J. P. [2008] “Dynamic topology in spatiotemporal chaos,” *Phys. Fluids* **20**, 064104.
- Pope, S. B., Yeung, P. K. & Girimaji, S. S. [1989] “The curvature of material surfaces in isotropic turbulence,” *Phys. Fluids A* **1**, 2010.
- Robinson, S. K. [1991] “Coherent motions in the turbulent boundary layer,” *Ann. Rev. Fluid Mech.* **23**, 601–639.
- Rypina, I. I., Brown, M. G., Beron-Vera, F. J., Kocak, H., Olascoaga, M. J. & Udovychenkov, I. A. [2007] “On the Lagrangian dynamics of atmospheric zonal jets and the permeability of the stratospheric polar vortex,” *J. Atmosph. Sci.* **64**, 3595–3610.
- Shadden, S. C., Lekien, F. & Marsden, J. E. [2005] “Definition and properties of Lagrangian coherent structures from finite-time Lyapunov exponents in two-dimensional aperiodic flows,” *Physica D* **212**, 271.
- Tallapragada, P. & Ross, S. D. [2013] “A set oriented definition of finite-time Lyapunov exponents and coherent sets,” *Commun. Nonlin. Sci. Numer. Simul.* **18**, 1106–1126.
- Thiffeault, J. L. & Allen, H. B. [2001] “Geometrical constraints on finite-time Lyapunov exponents in two and three dimensions,” *Chaos* **11**, 16–28.

- Thiffeault, J. L. [2002] “Derivatives and constraints in chaotic flows: Asymptotic behaviour and a numerical method,” *Physica D* **172**, 139–161.
- Thiffeault, J. L. [2004] “Stretching and curvature of material lines in chaotic flows,” *Physica D* **198**, 169–181.
- Xu, H., Ouellette, N. T. & Bodenschatz, E. [2007] “Curvature of Lagrangian trajectories in turbulence,” *Phys. Rev. Lett.* **98**, 050201.
- Yoo, T. S. [2004] *Insight into Images: Principles and Practice for Segmentation, Registration, and Image Analysis* (A K Peters/CRC Press).
- Zyczkowski, K. & Bollt, E. M. [1999] “On the entropy devil’s staircase in a family of gap-tent maps,” *Physica D* **132**, 392–410.